

Research article

Spontaneous regeneration of cholecystokinergic reticulospinal axons after a complete spinal cord injury in sea lampreys

Laura González-Llera^a, Gabriel N. Santos-Durán^a, Daniel Sobrido-Cameán^{a,1}, Carmen Núñez-González^b, Juan Pérez-Fernández^b, Antón Barreiro-Iglesias^{a,*}

^a Department of Functional Biology, CIBUS, Faculty of Biology, Universidade de Santiago de Compostela, 15782 Santiago de Compostela, Spain

^b CINBIO, Neurocircuits Group, Campus Universitario Lagoas, Marcosende, Universidade de Vigo, 36310 Vigo, Spain



ARTICLE INFO

Keywords:

Spinal cord injury
Axonal regeneration
Cholecystokinin
Synaptic vesicles
Lampreys
Locomotor performance

ABSTRACT

In contrast to humans, lampreys spontaneously recover their swimming capacity after a complete spinal cord injury (SCI). This recovery process involves the regeneration of descending axons. Spontaneous axon regeneration in lampreys has been mainly studied in giant descending neurons. However, the regeneration of neurochemically distinct descending neuronal populations with small-caliber axons, as those found in mammals, has been less studied. Cholecystokinin (CCK) is a regulatory neuropeptide found in the brain and spinal cord that modulates several processes such as satiety, or locomotion. CCK shows high evolutionary conservation and is present in all vertebrate species. Work in lampreys has shown that all CCKergic spinal cord axons originate in a single neuronal population located in the caudal rhombencephalon. Here, we investigate the spontaneous regeneration of CCKergic descending axons in larval lampreys following a complete SCI. Using anti-CCK-8 immunofluorescence, confocal microscopy and lightning adaptive deconvolution, we demonstrate the partial regeneration of CCKergic axons (81% of the number of axonal profiles seen in controls) 10 weeks after the injury. Our data also revealed a preference for regeneration of CCKergic axons in lateral spinal cord regions. Regenerated CCKergic axons exhibit colocalization with synaptic vesicle marker SV2, indicative of functional synaptic connections. We also extracted swimming dynamics in injured animals by using DeepLabCut. Interestingly, the degree of CCKergic reinnervation correlated with improved swimming performance in injured animals, suggesting a potential role in locomotor recovery. These findings open avenues for further exploration into the role of specific neuropeptidergic systems in post-SCI spinal locomotor networks.

1. Introduction

Spinal cord injuries (SCIs) pose significant challenges to humans and most non-human mammals, often resulting in irreversible damage to neural circuits and impaired motor function. One of the main causes of the lack of recovery of motor function after SCI is related to the incapacity of adult central nervous system (CNS) neurons to regenerate their axon after injury to reconnect with their appropriate targets (see [1]). The sea lamprey (*Petromyzon marinus* L.) offers a unique vertebrate model for studying axonal regeneration due to its remarkable ability to spontaneously recover from a complete SCI (see [2–4]). Axon regeneration research in lampreys has mainly relied on the study of individually identifiable giant descending neurons (e.g., [5–7]). These giant descending neurons of lampreys are located in the brainstem and project

their axons along the spinal cord. They offer a model system of great value both because they can be identified individually from brain to brain and because different giant descending neurons show very different regenerative abilities after SCI [5,8]. The use of these giant neurons as a model has provided important data on the role of different molecules and signalling pathways during spontaneous axon regeneration (e.g., [9–20]). However, similar giant neurons with large-caliber axons are not present in mammalian brains and the study of axon regeneration in giant neurons requires the use of neuronal tracers. Application of the tracer requires causing another retranssection of the spinal cord caudally to the site of the original injury and several additional days of recovery. So, it would be of great interest to analyse the regenerative ability of specific neuronal populations with small-caliber axons in lampreys and by using simpler immunohistochemical

* Corresponding author.

E-mail address: anton.barreiro@usc.es (A. Barreiro-Iglesias).

¹ Present address: Department of Zoology, University of Cambridge, Cambridge CB2 3EJ, UK

methods that do not involve tracer application. In the past, we, and others, used immunofluorescence methods to analyse the changes that occur in classical neurotransmitter systems with small-caliber axons after a complete SCI in lampreys (serotonin: [21]; dopamine: [22]; GABA: [23]; glutamate: [24]; glycine: [25]). However, using only neurotransmitter immunofluorescence methods, makes it difficult to distinguish between regenerated descending axons and axons coming from intrinsic spinal cord neurons. Among the diverse array of neural

populations impacted by SCI in lampreys, we have recently identified 2 descending neuropeptidergic systems [corticotropin releasing-hormone (CRH) and cholecystinin (CCK)] whose neurons are located in the lamprey brainstem [26,27]. These neuropeptidergic systems offer a model of value for the study of axon regeneration because in the lamprey spinal cord, there are no intrinsic CRHergic and CCKergic neurons, and all CRHergic and CCKergic axons are descending from the brainstem [26,27]. This allows to study the regeneration of small-caliber

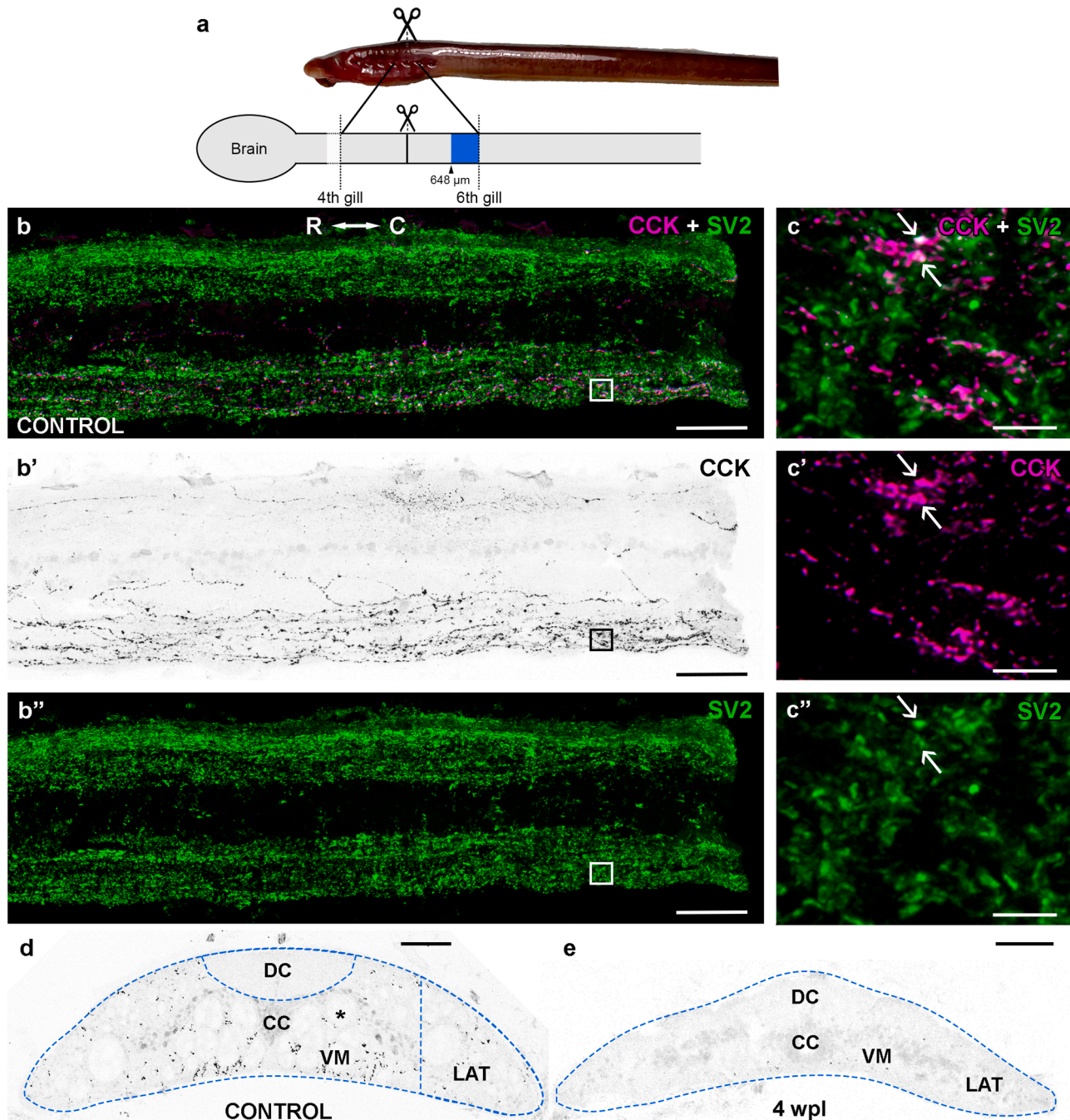


Fig. 1. CCK-ir axons are of descending origin and degenerate caudally to the injury site after axotomy. **a.** Lateral view of a sea lamprey larva and schematic drawing of a lateral view of the central nervous system indicating the site of SCI (scissors) and the area of axon quantification (blue). **b-b''.** Sagittal spinal cord section labelled with CCK (magenta or B&W) and SV2 (green) antibodies showing the longitudinal trajectory of descending CCK-ir axons. Note that CCK-ir axons are more abundant in the ventral region of the spinal cord (**b-b''**). **c.** Details of CCK-ir axons (square in **b-b''**) showing co-localization with SV2 (arrows). **d.** Transverse spinal cord section of a control larva showing the distribution of CCK-ir axons. **e.** Photomicrograph showing the absence of CCK-ir axons caudally to the site of SCI in a 4 wpl animal. Photomicrographs **b', d** and **e** with magenta (red) fluorescence were converted to B&W. Photomicrographs **c-c''** were taken with lightning adaptive deconvolution. **Fig. 1a** was taken from González-Llera et al. [28]. Abbreviations: C: caudal, CC: central canal, DC: dorsal column, LAT: lateral region, R: rostral, VM: ventromedial region. Scale bars, 50 µm (**b-b''**), 3 µm (**c-c''**), 75 µm (**d, e**).

descending neuropeptidergic axons by using simple immunofluorescence methods. Indeed, by using an antibody against the sea lamprey CRH mature peptide we have recently showed that by 10 weeks after a complete SCI at the level of the 5th gill, descending CRHergic axons of lampreys fully regenerate to at least the level of the 6th gill opening [28]. However, because CRHergic axons originate from 3 different neuronal populations of the brainstem [27], this neuropeptidergic system does not allow us to work with a single neurochemically distinct neuronal population as a model of spontaneous regeneration of small-caliber axons. In contrast, the CCKergic descending pathway originates from a single neuronal population located in the caudal rhombencephalon [26]. Moreover, the CCK-expressing descending pathway holds particular functional significance since this neuropeptidergic system plays a crucial role in lamprey locomotor circuits [29,30]. Despite its functional importance, the regenerative capacity of CCKergic axons of lampreys remains unexplored.

Here, we used an antibody generated against the sea lamprey CCK-8 mature peptide [26] to study the regenerative ability of descending CCKergic axons originating from the caudal rhombencephalon. We also performed analyses of swimming dynamics in 10 weeks post-lesion (wpl) animals to analyse the possible correlation between the degree of regeneration of CCKergic descending axons and the recovery of swimming ability. Our study offers a model system of value to study the spontaneous regeneration of small-caliber axons originating in a specific neuronal population by using simple immunofluorescence methods in lampreys.

2. Material and methods

2.1. Animals and SCI surgery

All animal experimental procedures were approved by the Committee of Bioethics at the University of Santiago de Compostela and the Xunta de Galicia government (Galicia, Spain; license number 15012/2020/011). Experiments with animals were performed in accordance with European Union and Spanish guidelines (Directive 2012–63-UE and RD 53/2013) on animal care and experimentation.

Mature larval sea lampreys, *Petromyzon marinus* L. ($n = 29$; more than 100 mm in body length, 5 to 7 years of age), were used in this study. Larvae were randomly assigned to the control or injury groups. Animals were deeply anesthetized with 0.1% tricaine methanesulfonate (MS-222; Sigma, St. Louis, MO, USA) in lamprey Ringer solution (137 mM NaCl, 2.9 mM KCl, 2.1 mM CaCl₂, 2 mM HEPES; pH 7.4) before experiments and euthanized by decapitation at the end of the experiments.

SCI surgeries were performed as described [31]. The spinal cord was exposed dorsally at the level of the 5th gill opening by making a longitudinal incision with a #11 scalpel. The complete spinal cord transection was performed with Spring scissors (Fine Science Tools, Heidelberg, Germany; Cat#15024–10). Completeness of the SCI was confirmed under the microscope by visualizing the spinal cord cut ends after surgery and was confirmed 24 h later by checking that there were no caudally propagating movements below the site of injury. After surgery, larvae were allowed to recover in individual tanks at 19.5°C for 4 or 10 weeks.

2.2. Behavioural analyses

Swimming performance of animals was qualitatively assessed at 10 wpl based on the scale of Ayers [32,33]. This assessment of swimming ability was made from video recordings of 5 min (Panasonic Full-HD camera HC-V110). The larvae were placed in an aquarium (36 × 23 × 10.5 cm) and, after 30 min of acclimatation, swimming activity was initiated by pinching the tail of the larva using a forceps. Swimming performance was categorized in a scale of 1 to 6 [32,33]. Animals in stages 5 to 6 are animals which axonal regeneration has occurred based on activity evoked by stimulation across the lesion site in the isolated

spinal cord [33]. Two blinded researchers evaluated each larva. Then, a mean value of swimming performance was generated for each larva.

To extract swimming dynamics from the same video recordings, we tracked the animals using DeepLabCut 2.3 [34], a Python software package that performs motion capture based on transfer learning with deep neural networks. The obtained data were analysed using custom written Matlab R2020b scripts. To analyse the videos, first three labels were placed in 40 frames chosen randomly from each video: one in the mouth, another in the neck, and the last one in the tip of the tail. Using the DeepLabCut *skeleton* function, two segments were created using these labels, one connecting the mouth and neck labels to extract the position of the head, and another connecting the neck and tail labels to extract the position of the body. The network was then trained, and once the training was evaluated, videos were analysed to extract the trajectories of the labels and the angles of the skeleton segments. In those cases in which insufficient labelling performance was observed, a refinement process was performed selecting outlier frames and refining the labels for additional rounds of training.

To determine the amplitude of swimming movements, first the body angle was calculated with respect to the head angle. Then, the body position was plotted over time and the Matlab function *findpeaks* was used to extract the maximum amplitudes in both directions (right and left respect to the body midline). Amplitudes were determined by calculating the angle for each swimming cycle respect to the midline (see Supplementary Video 1). The analysis was done isolating events from the original 5 min videos in which the animals were swimming straight, until reaching a total of 30 s analysed per animal, so that turning events that would impact on the obtained amplitudes were avoided. The total duration of swimming behaviour analysed was determined by the amount of swimming events that could be extracted in animals with low swimming performance. Swimming frequency was calculated dividing the number of swimming cycles by time. To calculate the distance travelled and the speed, the position of the head in the X and Y axes was extracted during a continuous swimming event of 1 min, and the distance travelled between adjacent frames was calculated using the arc length formula. The instant velocity was calculated by dividing the distance travelled between adjacent frames by time. Total distance in the 1-minute swimming event was calculated by summing the individual arc distances, and velocity was determined by dividing the travelled distance by time. The length of the swimming chamber was compared to its video image in pixels to provide a reliable conversion index so that the distance travelled could be translated into centimetres.

Supplementary material related to this article can be found online at [doi:10.1016/j.csbj.2023.12.014](https://doi.org/10.1016/j.csbj.2023.12.014).

2.3. Immunofluorescence in spinal cord sections

The spinal cord between the 4th and 6th gills (Fig. 1a) was dissected and fixed by immersion in 4% paraformaldehyde (PFA) in 0.05 M Tris-buffered saline pH 7.4 (TBS) for 6 h at 4 °C. The spinal cord was then rinsed in TBS, cryoprotected in 30% sucrose in TBS overnight at 4°C, embedded in Neg-50 (Epredia; Portsmouth, New Hampshire, USA), frozen in liquid nitrogen, and cut on a cryostat (18 µm; sagittal or transverse sections). Sections were mounted on Superfrost® Plus glass slides (ThermoFisher Scientific; Waltham, MA, USA). Then, they were incubated with mixture of a purified rabbit polyclonal anti-sea lamprey CCK-8 antibody (dilution 1:200; [26]; see Section 2.4) and a mouse monoclonal anti-synaptic vesicle 2 (SV2) glycoprotein antibody (1:250; Developmental Hybridoma Bank, University of Iowa, Iowa, USA; RRID: AB_2315387) at RT overnight. After washes in TBS, the sections were incubated for one hour at RT with a mixture of a Cy3-conjugated goat anti-rabbit antibody (1:500; Millipore, Burlington, MA; Cat# AP132C; RRID: AB_92489) and a FITC-conjugated goat anti-mouse antibody (1:200; Invitrogen, Carlsbad, CA; Cat# F2761; RRID: AB_2536524). Antibodies were prepared in a solution containing 15% normal goat serum and 0.2% Triton as a detergent. Sections were then rinsed in TBS

and distilled water and mounted with Mowiol (Sigma).

2.4. Specificity of primary antibodies

The anti-CCK antibody was generated by Biomedal (Sevilla, Spain) against the mature sea lamprey CCK-8 peptide (CDY(SO₃)IGWMDFNH₂) modified with the addition of a cysteine (C) to the N-terminus. The C was introduced to allow coupling of the peptide to key limpet hemocyanin (KLH). An 8 weeks old rabbit (New Zealand White) was immunized subcutaneously with 400 mg of the peptide-KLH conjugate emulsified in Freund's complete adjuvant. After 4 weeks, the rabbit was immunized once a week for 2 weeks via intramuscular injections (200 mg). Pre-immune and post-immunization bleeds were collected. 2.5 mL of antiserum from the final bleed were purified using a protein A-Sepharose column (GE Healthcare, Little Chalfont, UK).

The purified fraction of the anti-CCK antibody was tested for specificity with an ELISA [26]. The purified antibody (at concentrations from 1:1000 to 1:100000) and the pre-immune serum (1:1000) were tested against the synthetic CCK-8 peptide without KLH (1 mM). The purified antibody gave a positive signal at all the tested concentrations, while the very low signal registered with the pre-immune serum (no anti-CCK antibodies present) was the same as the one obtained in negative controls with saline only [26]. The pattern of CCK-immunoreactive (-ir) neuronal populations in the CNS matches the pattern of expression of the CCK mRNA observed by in situ hybridization [26].

The anti-SV2 antibody was generated against purified synaptic vesicles of the electric ray [35]. The antibody recognizes the 3 SV2 isoforms (A to C) and labels synaptic vesicle clusters in all tested vertebrates, including lampreys [9,28,36–39].

2.5. Imaging and quantification

Two different types of confocal microscopes (TCS-SP2 or Stellaris 8; Leica, Wetzlar, Germany) were used to acquire images of the spinal cord sections. Optical sections were taken at steps of 2.5 (Leica TCS-SP2) or 0.7 (Leica Stellaris 8) μm along the z-axis when using the 20x objective and at steps of 0.3 μm when using the 40x/63x objectives. Lightning adaptive deconvolution was used to obtain maximum resolution [40] in some double labelling images obtained with the Leica Stellaris 8 confocal microscope (40x or 63x objectives). Collapsed projections of spinal cord sections (18 μm) were obtained with the LITE software or LAS X software (Leica). Figures were generated using Adobe Photoshop 2022 (Adobe, San Jose, CA, USA). Confocal photomicrographs from the red channel were converted to magenta or B&W in the figures to facilitate viewing. Schematic drawings were obtained from a previous publication (Fig. 1a; [28]).

CCK-ir axonal profiles were quantified in photomicrographs of transverse sections using the Feature J plugin of the Fiji software (see [41]). The images from control and 10 wpl animals were taken with the same confocal microscope (Leica TCS-SP2; 20x objective) and using the same parameters. A threshold was determined to obtain the most

accurate images when converting them to binary B&W images for profile quantification. We quantified the number of CCK-ir axonal profiles in 1 out of every 4 consecutive spinal cord sections starting at the level of the 6th gill opening and moving rostrally. We also quantified separately the number of CCK-ir axonal profiles in both lateral regions of the spinal cord. To delimit the lateral areas, we used as a limit the giant axons of the ventromedial region of the spinal cord. 9 sections were analysed per animal covering 648 μm of spinal cord below the site of injury (Fig. 1a). The mean number of CCK-ir axonal profiles per section was obtained for each animal based on the quantification of the 9 sections (each data point in the graphs represents one larva).

2.6. Statistical analyses

Statistical analyses were carried out with Prism 9 (GraphPad, La Jolla, CA, USA). We first checked the data for normality using the D'Agostino-Pearson test. In order to assess any significant differences (with $p \leq 0.05$) between the control group and the animals at 10 weeks post-lesion (10 wpl), we used a two-tailed unpaired Student's t-test, assuming the data followed a normal distribution based on the results from the D'Agostino-Pearson test. Each experimental group, consisting of a minimum of 10 animals, was obtained from three separate batches of animals. For each batch, the control and 10 wpl animals were always processed in parallel.

To determine possible correlations between 2 measured parameters (CCK-ir axonal profiles, swimming frequency, swimming amplitude, distance, or velocity) we used a simple linear regression. We determined the significance of the slope with respect to zero ($p \leq 0.05$) and calculated the equation of the straight line and the R².

3. Results and discussion

Previous immunofluorescence and in situ hybridization experiments revealed that the spinal cord of mature larval sea lampreys only contains CCK-ir axons and no intrinsic CCKergic neurons (immunofluorescence and in situ hybridization data; [26]; Fig. 1b-d). Tract-tracing experiments with the tracer Neurobiotin (applied at the level of the 5th gill) revealed that all the spinal cord CCK-ir axons originate in a single CCK-ir cell population located in the caudal rhombencephalon [26].

In the present study, we first carried out double immunofluorescence experiments against CCK and SV2 in sagittal spinal cord sections at the level of the 6th gill in non-injured animals. These sagittal sections revealed a system of CCK-ir axons coursing with descending longitudinal trajectories in the spinal cord (Fig. 1b-b'). As can be observed in these sections, CCK-ir axons are more abundant in the ventral portion of the spinal cord (Fig. 1b-b'). Double labelling with anti-SV2 antibodies (synaptic vesicle marker) revealed colocalization of CCK and SV2 immunofluorescence in the same axons, which shows that CCK-ir descending fibres establish pre-synaptic contacts in their descending course along the spinal cord (Fig. 1b-c'). Transverse spinal cord sections at the same spinal cord level revealed that most CCK-ir axons are located

Table 1

Data from 10 wpl animals. Lampreys were numbered in ascending order based on the number of regenerated CCK-ir axonal profiles per section.

	Ayer's scale	CCK-ir [# axonal profiles/section]	Distance [cm]	Velocity [cm/s]	Frequency [Hz]	Amplitude [°]
Lamprey 1	5.5	164.750	438.033	7.205	5.950	8.330
Lamprey 2	5.5	268.778	1078.690	17.859	12.103	7.553
Lamprey 3	4	270.167	425.443	6.978	7.975	9.694
Lamprey 4	4.5	270.625	400.021	6.623	8.531	5.932
Lamprey 5	4	282.286	736.807	12.139	8.253	8.701
Lamprey 6	5.5	289.500	627.982	10.992	9.318	6.017
Lamprey 7	5.5	318.333	741.932	12.250	11.923	4.041
Lamprey 8	4	320.286	994.610	16.513	11.641	5.949
Lamprey 9	6	335.556	800.667	13.183	11.799	6.155
Lamprey 10	4	357.875	884.044	14.685	10.200	6.995
Lamprey 11	5.5	359.714	548.215	9.076	8.716	5.456

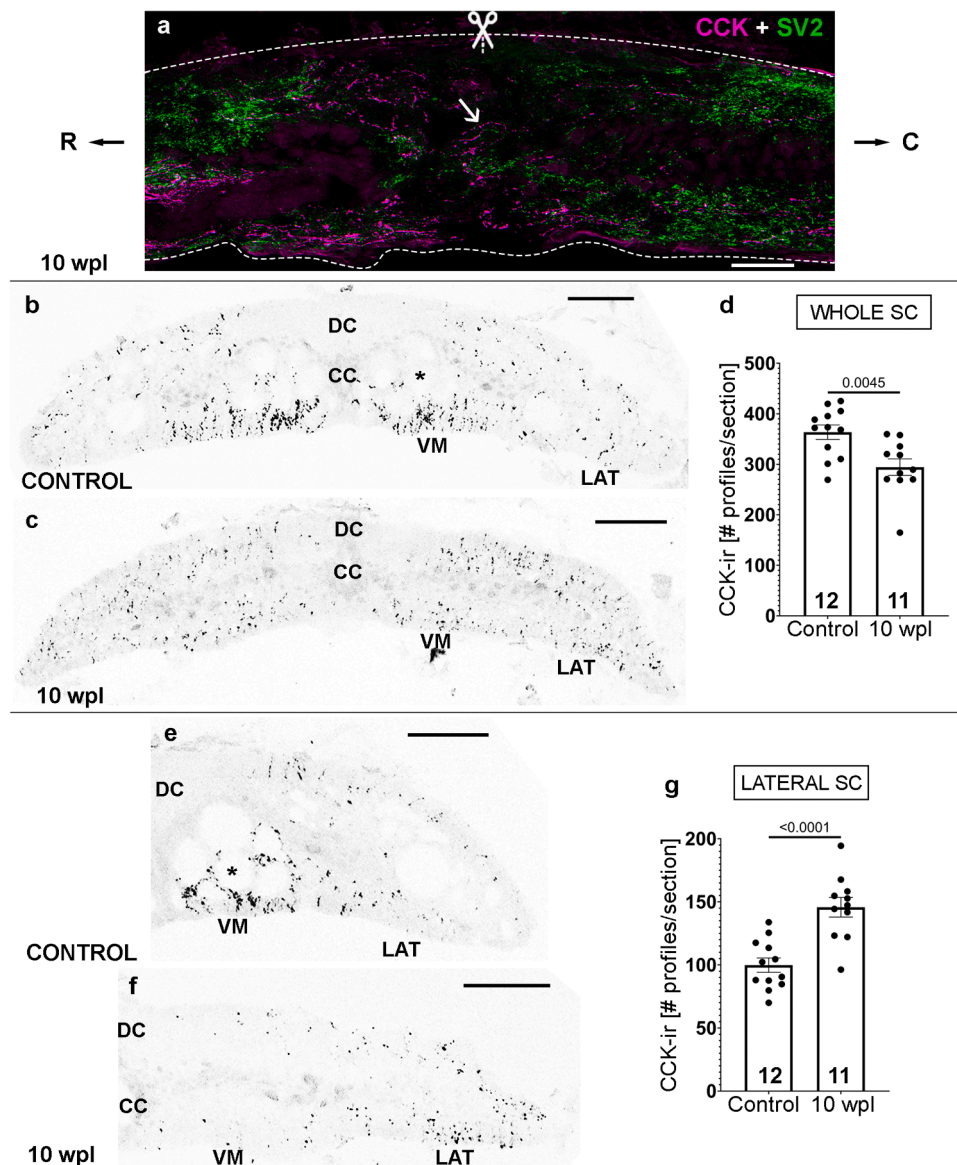


Fig. 2. Partial regeneration of CCK-ir axons in 10 wpl animals. **a.** Sagittal section of the injury site (level of the 5th gill; scissors) of a 10 wpl animal labelled with CCK and SV2 antibodies. Note the low level of SV2 expression. Regenerated CCK-ir axons crossing the injury site into the caudal portion are indicated with an arrow. **b, c.** Transverse spinal cord sections of control (**b**) and 10 wpl (**c**) larvae (level of the 6th gill) showing that numbers of CCK-ir axonal profiles in 10 wpl animals were significantly lower than those of un-injured controls (see graph in **d**, each dot represents 1 animal). **e, f.** Lateral region of control (**e**) and 10 wpl (**f**) spinal cords at the level of the 6th gill showing that the number of CCK-ir axonal profiles is significantly higher in this region in 10 wpl animals (see graph in **g**, each dot represents 1 animal). Photomicrographs **b, c, e** and **f** with magenta (red) fluorescence were converted to B&W. For abbreviations, see **Fig. 1** legend. Scale bars, 50 μ m (**a**), 75 μ m (**b, c**), 65 μ m (**e, f**).

in its ventromedial region, with some axons being located also in the dorsolateral and lateral regions (**Fig. 1d**). No CCK-ir axons were present in the dorsal column (**Fig. 1d**). To analyse the response of CCKergic axons to axotomy, we first analysed animals at 4 weeks after a complete SCI at the level of the 5th gill. The point of this experiment is that intraspinal or ascending axons coming from intrinsic CCK-ir neurons could remain caudally to the site of a complete SCI, but descending axons disconnected from their neuronal somas would degenerate in the caudal portion. Indeed, the spinal cord of 4 wpl animals was depleted of CCK-ir axons below the site of SCI (at the level of the 6th gill opening; **Fig. 1e**). It should be noted that tracer labelling in lampreys has shown that some small axons bridge the lesion site by 2 weeks post-SCI [42] and that these early regenerating axons come from both propriospinal and small reticulospinal neurons [43]. Our data indicates that this is not the case for descending CCKergic axons, which are not present below the site of injury (at the level of the 6th gill opening) at 4 wpl. Taken

together, previous [26] and present data reveal that all CCK-ir axons present at the level of the 5th/6th gill openings are descending axons that degenerate caudally (level of the 6th gill) to the site of injury (level of the 5th gill) within the first 4 wpl.

Based on these data, we decided to analyse the regenerative capacity of axotomized CCK-ir axons after a complete spinal cord transection. We choose the 10 wpl time point because previous work has shown that 10 wpl larvae present a high degree of swimming recovery [28,44–46] and axon regeneration [5,11,28,47] after a transection SCI at the level of the 5th gill. 10 wpl animals ($n = 11$) showed a mean value of 4.9 ± 0.24 in Ayer's scale (minimum of 4 with 55% of the larvae between 5 and 6; these 10 wpl animals are the same animals in which we studied the regeneration of CRHergic axons in a previous study in a different set of spinal cord cryostat sections [28]; **Table 1**). At level 4 in the Ayer's scale, rostro-caudal undulatory movements become coordinated and propagating waves travel along the body, which is suggestive of the recovery

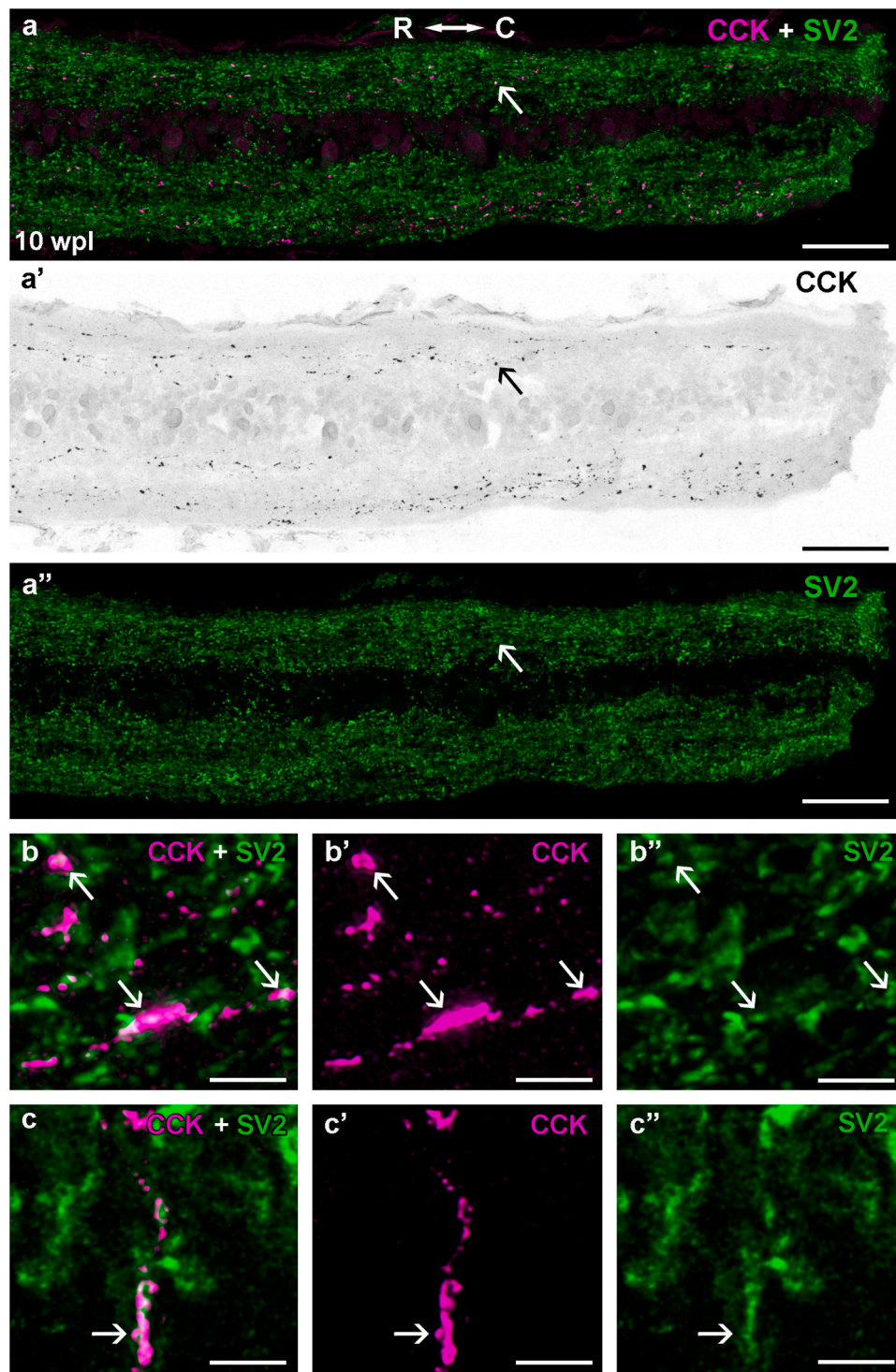


Fig. 3. Photomicrographs showing regenerated CCK-ir axons at 10 wpl. a-a''. Sagittal spinal cord sections labelled with anti-CCK and anti-SV2 antibodies. b-c''. Details of regenerated CCK-ir axons in sagittal (b-b'') and transverse (c-c'') sections showing co-localization of CCK and SV2 immunofluorescences (arrows). Photomicrograph a' with magenta (red) fluorescence was converted to B&W. Photomicrographs b-b'' and c-c'' were taken with lightning adaptive deconvolution. For abbreviations, see Fig. 1 legend. Scale bars, 50 μm (a-a''), 3 μm (b-b'', c-c'').

of intersegmental coordination related to axon regeneration. However, animals in stage 4, in contrast to level 5/6 animals, usually exhibit a bilateral asymmetry of curvature on one side during swimming, which leads to an incapacity to maintain the typical dorsal-side-up orientation all the time.

Sagittal sections at the lesion site (at the level of the 5th gill) of 10 wpl animals showed regenerated CCK-ir descending axons crossing the

site of SCI and reinnervating the caudal portion of the spinal cord (for an example, see arrow in Fig. 2a). The site of SCI can be identified by the disorganization of the tissue around the injury and also due to the absence of intense SV2 labelling (Fig. 2a). We quantified the degree of regeneration of CCK-ir axons in transverse sections of the spinal cord at the level of the 6th gill (below the site of injury). This revealed a high but partial regeneration (approximately 81%) of the number of CCK-ir

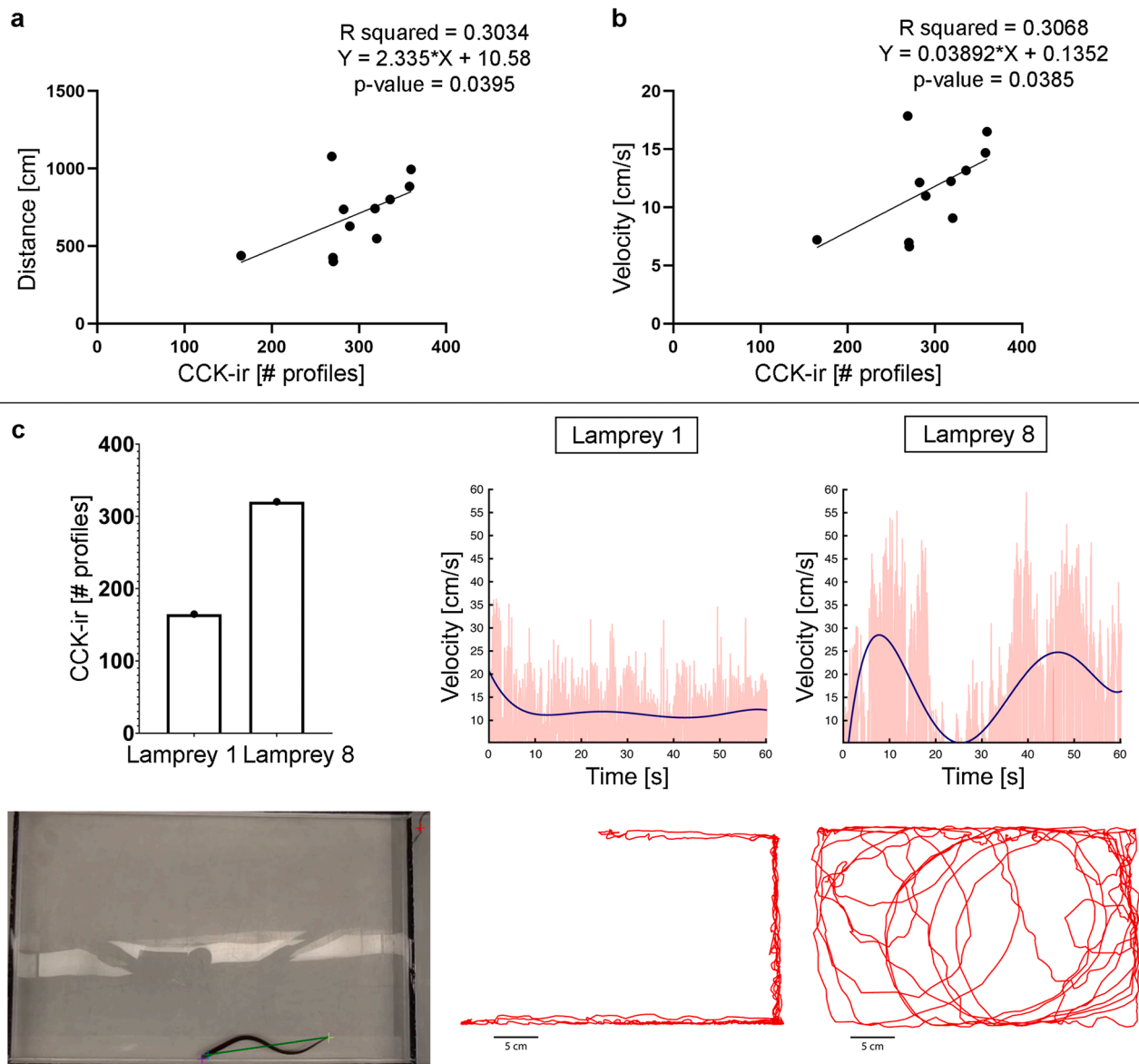


Fig. 4. Positive correlation between the number of CCK-ir axonal profiles and recovery of locomotion (swimming distance and velocity). a. Graph showing a positive correlation (simple linear regression) between swimming distance and the number of CCK-ir axonal profiles of 10 wpl animals. b. Graph showing a positive correlation (simple linear regression) between swimming velocity and the number of CCK-ir axonal profiles of 10 wpl animals. c. Examples of the swimming performance of two 10 wpl lampreys (lampreys 1 and 8 in Table 1) with low and high numbers of regenerated CCK-ir axonal profiles. Numbers of axonal profiles of lampreys 1 and 8 are indicated to the top left. A representative frame showing an animal in the swimming chamber with the labels (colored crosses) and the segments (green lines) used to extract swimming dynamics is shown to the bottom left (the red label is used to extract possible camera movements). Top graphs in the right represent the velocity between adjacent frames (red line), and the data fitted with a 5th degree polynomial (blue line) during a minute of swimming, whose trajectories are shown below for each lamprey. Fitting equations: Lamprey 1: $y = -6.141e^{-07} \cdot x^2 + 0.0001056 \cdot x^4 - 0.006647 \cdot x^3 + 0.1878 \cdot x^2 - 2.336x + 16.76$; Lamprey 8: $y = 3.941e^{-06} \cdot x^5 - 0.0006846 \cdot x^4 + 0.04245 \cdot x^3 - 1.106 \cdot x^2 + 10.7x + 5.356$.

axonal profiles observed in control animals (control: 363.6 ± 49.58 axonal profiles/section; 10 wpl: 294.4 ± 54.79 axonal profiles/section; Fig. 2b-d). Numbers of regenerated CCK-ir axonal profiles at 10 wpl were significantly lower than the number of CCK-ir axonal profiles of control animals (Unpaired t-test, $p = 0.0045$; Fig. 2b-d). These results reveal that CCKergic descending axons of lampreys spontaneously regenerate after a complete SCI. These CCK-ir axons correspond to descending regenerated axons because 10 wpl animals show no intrinsic spinal cord CCK-ir neurons as control non-injured animals. This indicates that CCKergic neurons are not newly generated after injury in the sea lamprey spinal cord, and that there is no change in transmitter phenotype from pre-existing neurons as previously shown in rodent neurons switching between glutamatergic and GABAergic phenotypes

after SCI [48].

It should be noted that the descending CCKergic system does not completely recover the degree of innervation seen at the level of the 6th gill in control animals (81% of the original innervation). This is in marked contrast with descending CRHergic axons, which, in the same animals, regenerate completely at this spinal cord level [28]. Thus, different descending neuropeptidergic neurons of lampreys show different regenerative abilities after SCI. This also occurs with the different axonal regenerative abilities observed between individual giant descending neurons ([5], see [2]). Future single cell RNAseq experiments, as those recently performed to generate an atlas of cell types of the lamprey brain [49], could help in determining possible cell heterogeneity within the descending CCKergic population in relation to

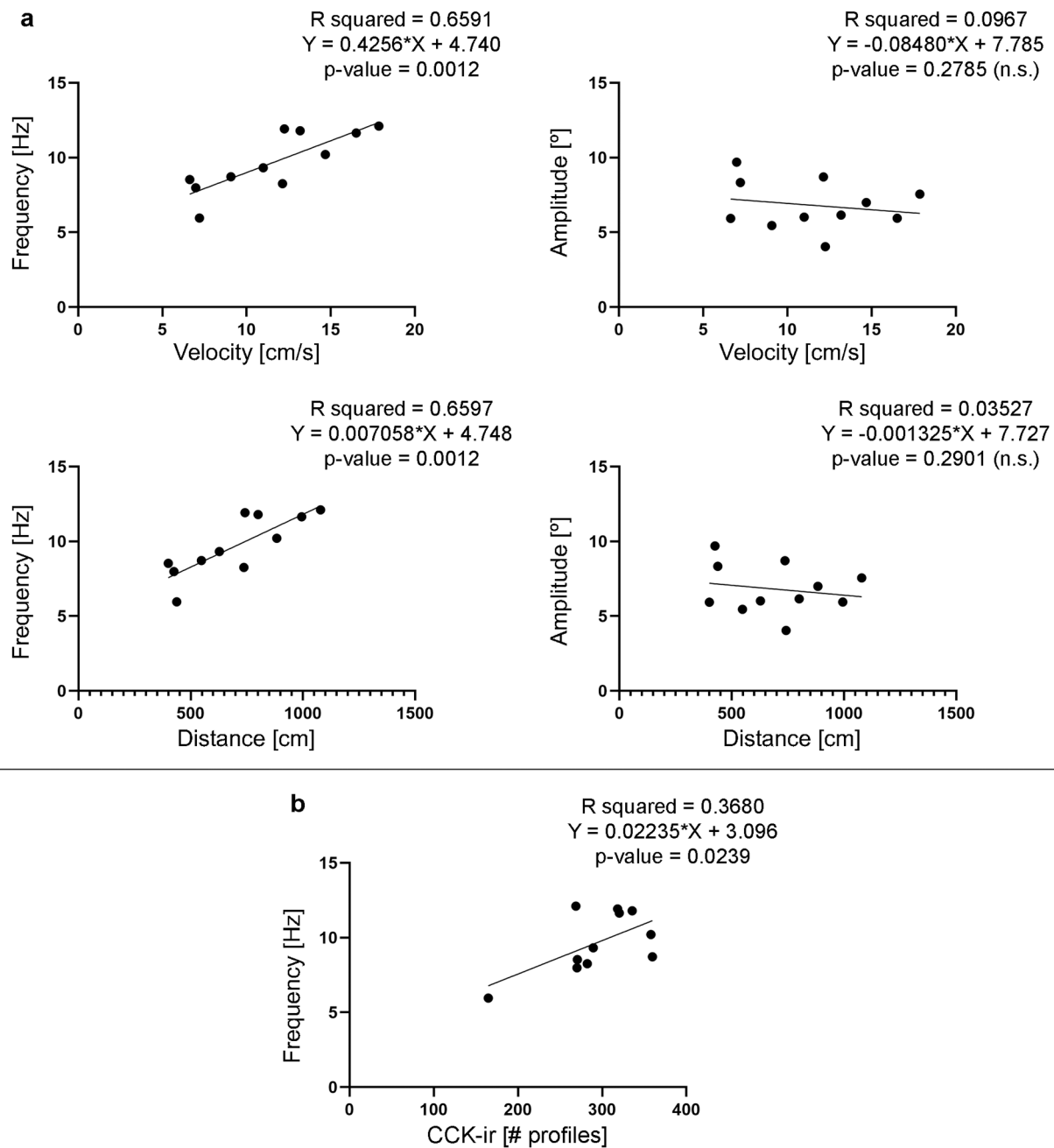


Fig. 5. Recovered animals show a positive correlation of swimming frequency (but not amplitude) with swimming distance and velocity. a. Graphs showing a positive correlation (simple linear regression) between swimming frequency and swimming distance or velocity and the lack of correlation between swimming amplitude and swimming distance or velocity in 10 wpl animals. b. Graph showing a positive correlation (simple linear regression) between swimming frequency and the number of CCK-ir axonal profiles in 10 wpl animals.

their regenerative ability. As far as we know, this is the first report showing spontaneous regeneration of CCKergic axons in the spinal cord of any vertebrate, only a previous study revealed spontaneous regeneration of CCKergic retinofugal axons into the optic tectum of *Rana pipens* after a unilateral crush injury to the optic nerve [50].

While quantifying the numbers of CCK-ir axonal profiles in 10 wpl animals we noticed a possible change in the distribution of the CCK-ir axons in regenerated animals. In 10 wpl animals, regenerated CCK-ir axons appeared to be more abundant in the lateral portion of the spinal cord than in controls, while the density of CCK-ir axons seemed to be lower in the ventromedial region (Fig. 2e, f). Indeed, quantification of the number of CCK-ir axonal profiles only in the lateral portion of the cord revealed a significant increase in CCK-ir innervation in this region

(control: 99.83 ± 5.66 axonal profiles; 10 wpl: 145.7 ± 7.78 axonal profiles; Unpaired t-test, $p < 0.0001$; Fig. 2g), even despite the reduced re-innervation seen in the whole spinal cord (see above; Fig. 2b-d). This reveals that the CCKergic descending system is highly plastic and regenerates preferentially in the lateral region of the cord. Interestingly, giant descending neurons whose axons run in the dorsolateral or lateral regions of the spinal cord also show better survival and regenerative abilities than giant descending neurons whose axons run on the ventromedial region of the spinal cord ([51]; Fernández-López et al., 2008). Thus, previous and present data suggest that the lateral portion of the spinal cord could be more permissive for axonal regeneration than the ventromedial region. Previous studies have reported the expression of axonal guidance receptors and their ligands in identifiable descending

neurons and in the spinal cord of lampreys and changes in their expression after a complete SCI (semaphorins: [52]; neurotrophins/tropomyosin-related kinase receptors: [53]; UNC-5: [6, 54,55]; neogenin/RGM: [6,12,56,31,57]; plexinA: [6]). The descending CCKergic system now offers a model of interest to study the preferential regrowth and guidance of small-caliber descending axons in specific spinal cord regions and the role of axonal guidance molecules in this process.

Double immunofluorescence experiments in spinal cord sections at the level of the 6th gill showed colocalization of CCK and SV2, which indicates the presence of synaptic vesicle clusters and possible synapse regeneration in regenerated CCK-ir axons below the site of SCI (Fig. 3). This colocalization data suggest that the regrowth of CCK-ir axons could have an impact on functional recovery of 10 wpl animals. As indicated above, all animals showed a good recovery of their swimming ability based on qualitative assessments with the Ayer's scale (4 or higher). But for a more quantitative way of evaluating the locomotor performance of 10 wpl larvae we decided to extract their swimming dynamics from video recordings using DeepLabCut 2.3 [34]. As can be observed in Table 1, we detected different degrees of recovery in the different 10 wpl larvae based on their swimming distance and mean swimming velocity during 1 min. Importantly, we found positive correlations between the numbers of regenerated CCK-ir axonal profiles and the parameters of distance or velocity (Fig. 4). Recent work has shown that transected larval lampreys increase their wave frequencies to swim faster (i.e., transected lampreys have higher frequencies than control lampreys with similar velocities) and that they have lower amplitudes than control animals [58]. In the same sense, in our data we also observed a positive correlation between frequency and velocity in injured animals but no correlation between amplitude and velocity (Fig. 5a). Interestingly, we also observed a positive correlation between wave frequency and the numbers of regenerated CCK-ir axonal profiles (Fig. 5b). CCK-ir reticular cells projecting to the spinal cord are part of the lamprey locomotor circuits [29,30] and spinal cord motor neurons and large sensory cells have many close appositions to CCK varicosities from descending CCKergic axons [29]. So, our SV2 colocalization and behavioural data suggest that regenerated CCKergic axons could be functional and contribute to the recovery of swimming ability in lampreys. Future work using electrophysiology, specific tract-tracing or CCK knockdown (e.g., by using morpholinos; see [59]) could allow to dissect the role of CCK in the regenerated locomotor network and could reveal a true "cause-effect" between the regeneration of CCKergic axons and locomotion. Recovery of swimming performance in lampreys is not simply the reconnection of the two sides of the spinal cord but includes a variety of changes in the spinal networks including changes in the cellular and synaptic properties (the "new spinal cord hypothesis"; [4]). Our data also reveals plastic changes in the regenerated CCKergic descending system (incomplete regeneration and reroute of axons to lateral regions of the cord) that might contribute to the recovery of swimming in lesioned animals. This reroute of regenerated CCKergic axons to the lateral areas of the spinal cord is of interest because previous work has shown that the lateral spinal tracts of non-injured lampreys contain a significant part of the descending command pathway for locomotion [60].

4. Conclusions

Our work provides a unique model to understand spontaneous and functional regeneration of small-caliber axons from a specific neuro-peptidergic population in lampreys by using simple immunofluorescence methods. Previous work in lampreys has focused on the study of giant neurons by means of tracer applications (e.g., [6,9,11,15,18]). More recently, we studied the regeneration of descending CRHergic axons [28], which originate in 3 different cell populations of the lamprey brainstem [27]. Differences with the complete regeneration observed in the CRHergic descending system provide an opportunity to

search for the genes and signalling molecules that determine complete vs incomplete regeneration of small-caliber axons in lampreys by comparing both neuropeptidergic systems. Changes in the distribution of regenerated CCKergic axons after SCI are also of interest to study the role that this plasticity has in functional recovery. These findings contribute to our understanding of the complex mechanisms underlying functional recovery after SCI in lampreys and open avenues for further exploration into the role of specific neuro-peptidergic systems in post-SCI spinal locomotor networks.

Funding

Grant PID2020–115121 GB-I00 funded by MCIN/AEI/10.13039/501100011033 to A. Barreiro-Iglesias. Grant ED431C 2021/18 funded by Xunta de Galicia. Long-term EMBO fellowship ALTF 62–2021 to D.S.-C. by European Molecular Biology Organization. The Ramón y Cajal grant RYC2018–024053-I funded by MCIN/AEI/ 10.13039/501100011033 and by "ESF Investing in your Future" to J.P.-F. Xunta de Galicia (ED431B 2021/04 to J.P.-F. and ED481A 2022/433 to C.N.-G).

CRediT authorship contribution statement

Laura González-Llera: Investigation, Methodology, Writing – review & editing. **Gabriel N. Santos-Durán:** Investigation, Methodology. **Daniel Sobrido-Cameán:** Investigation, Methodology, Writing – review & editing. **Carmen Núñez-González:** Investigation, Methodology. **Juan Pérez-Fernández:** Investigation, Methodology, Writing – original draft, review & editing. **Antón Barreiro-Iglesias:** Conceptualization, Writing – original draft, review & editing, Supervision, Funding acquisition.

Declaration of Competing Interest

The authors declare that they have no known competing financial interests or personal relationships that could have appeared to influence the work reported in this paper.

Acknowledgements

The authors would like to thank the staff of Ximonde Biological Station for providing the larval lampreys, and the Microscopy Service (University of Santiago de Compostela) and Dr. Mercedes Rivas Cascallar for confocal microscope facilities and help.

References

- [1] Zheng B, Tuszynski MH. Regulation of axonal regeneration after mammalian spinal cord injury. *Nat Rev Mol Cell Biol* 2023;24.
- [2] Rodicio MC, Barreiro-Iglesias A. Lampreys as an animal model in regeneration studies after spinal cord injury. *Rev Neurol* 2012;55. <https://doi.org/10.33588/rn.5503.2012136>.
- [3] Barreiro-Iglesias A. Bad regenerators die after spinal cord injury: insights from lampreys. *Neural Regen Res* 2015;10. <https://doi.org/10.4103/1673-5374.150642>.
- [4] Parker D. The lesioned spinal cord is a "new" spinal cord: evidence from functional changes after spinal injury in lamprey. *Front Neural Circuits* 2017;11. <https://doi.org/10.3389/fncir.2017.00084>.
- [5] Jacobs AJ, Swain GP, Snedeker JA, Pijak DS, Gladstone LJ, Selzer ME. Recovery of neurofilament expression selectively in regenerating reticulospinal neurons. *J Neurosci* 1997;17. <https://doi.org/10.1523/jneurosci.17-13-05206.1997>.
- [6] Chen J, Laramore C, Shifman MI. The expression of chemorepulsive guidance receptors and the regenerative abilities of spinal-projecting neurons after spinal cord injury. *Neurosci* 2017;26. <https://doi.org/10.1016/j.neuroscience.2016.11.020>.
- [7] Jin LQ, Zhou Y, Li YS, Zhang G, Hu J, Selzer ME. Transcriptomes of injured lamprey axon tips: single-cell RNA-Seq suggests differential involvement of mapk signaling pathways in axon retraction and regeneration after spinal cord injury. *Cells* 2022;11. <https://doi.org/10.3390/cells11152320>.
- [8] Sobrido-Cameán D, Barreiro-Iglesias A. Role of caspase-8 and Fas in cell death after spinal cord injury. *Front Mol Neurosci* 2018;11. <https://doi.org/10.3389/fnmol.2018.00101>.

- [9] Lau BYB, Fogerson SM, Walsh RB, Morgan JR. Cyclic AMP promotes axon regeneration, lesion repair and neuronal survival in lampreys after spinal cord injury. *Exp Neurol* 2013;250. <https://doi.org/10.1016/j.expneurol.2013.09.004>.
- [10] Herman PE, Papatheodorou A, Bryant SA, Waterbury CKM, Herdy JR, Arcese AA, et al. Highly conserved molecular pathways, including Wnt signaling, promote functional recovery from spinal cord injury in lampreys. *Sci Rep* 2018;8. <https://doi.org/10.1038/s41598-017-18757-1>.
- [11] Romaus-Sanjurjo D, Ledo-García R, Fernández-López B, Hanslik K, Morgan JR, Barreiro-Iglesias A, et al. GABA promotes survival and axonal regeneration in identifiable descending neurons after spinal cord injury in larval lampreys. *Cell Death Dis* 2018;9. <https://doi.org/10.1038/s41419-018-0704-9>.
- [12] Chen J, Shifman MI. Inhibition of neogenin promotes neuronal survival and improved behavior recovery after spinal cord injury. *Neuroscience* 2019;408. <https://doi.org/10.1016/j.neuroscience.2019.03.055>.
- [13] Rodemer W, Selzer ME. Role of axon resealing in retrograde neuronal death and regeneration after spinal cord injury. *Neural Regen Res* 2019;14.
- [14] Rodemer W, Zhang G, Sinita I, Hu J, Jin LQ, Li S, Selzer ME. PTP α knockdown in lampreys impairs reticulospinal axon regeneration and neuronal survival after spinal cord injury. *Front Cell Neurosci* 2020;14. <https://doi.org/10.3389/fncel.2020.00061>.
- [15] Sobrido-Cameán D, Robledo D, Sánchez L, Rodicio MC, Barreiro-Iglesias A. Serotonin inhibits axonal regeneration of identifiable descending neurons after a complete spinal cord injury in lampreys. *DMM Dis Model Mech* 2019;12. <https://doi.org/10.1242/dmm.037085>.
- [16] Sobrido-Cameán D, Fernández-López B, Pereiro N, Lafuente A, Rodicio MC, Barreiro-Iglesias A. Taurine promotes axonal regeneration after a complete spinal cord injury in lampreys. *J Neurotrauma* 2020;37. <https://doi.org/10.1089/neu.2019.6604>.
- [17] Sobrido-Cameán D, Robledo D, Romaus-Sanjurjo D, Pérez-Cedron V, Sánchez L, Rodicio MC, et al. Inhibition of gamma-secretase promotes axon regeneration after a complete spinal cord injury. *Front Cell Dev Biol* 2020;8. <https://doi.org/10.3389/fcell.2020.00173>.
- [18] Hu J, Zhang G, Rodemer W, Jin LQ, Shifman M, Selzer ME. The role of RhoA in retrograde neuronal death and axon regeneration after spinal cord injury. *Neurobiol Dis* 2017;98. <https://doi.org/10.1016/j.nbd.2016.11.006>.
- [19] Hu J, Rodemer W, Zhang G, Jin LQ, Li S, Selzer ME. Chondroitinase ABC promotes axon regeneration and reduces retrograde apoptosis signaling in lamprey. *Front Cell Dev Biol* 2021;9. <https://doi.org/10.3389/fcell.2021.653638>.
- [20] Hu J, Jin LQ, Selzer ME. Inhibition of central axon regeneration: perspective from chondroitin sulfate proteoglycans in lamprey spinal cord injury. *Neural Regen Res* 2022;17. <https://doi.org/10.4103/1673-5374.335144>.
- [21] Cohen AH, Abdelnabi M, Guan L, Ottinger MA, Chakrabarti L. Changes in distribution of serotonin induced by spinal injury in larval lampreys: evidence from immunohistochemistry and HPLC. *J Neurotrauma* 2005;22. <https://doi.org/10.1089/neu.2005.22.172>.
- [22] Fernández-López B, Romaus-Sanjurjo D, Cornide-Petronio ME, Gómez-Fernández S, Barreiro-Iglesias A, Rodicio MC. Full anatomical recovery of the dopaminergic system after a complete spinal cord injury in lampreys. *Neural Plast* 2015;2015. <https://doi.org/10.1155/2015/350750>.
- [23] Romaus-Sanjurjo D, Valle-Maroto SM, Barreiro-Iglesias A, Fernández-López B, Rodicio MC. Anatomical recovery of the GABAergic system after a complete spinal cord injury in lampreys. *Neuropharmacology* 2018;131. <https://doi.org/10.1016/j.neuropharm.2018.01.006>.
- [24] Fernández-López B, Barreiro-Iglesias A, Rodicio MC. Anatomical recovery of the spinal glutamatergic system following a complete spinal cord injury in lampreys. *Sci Rep* 2016;6. <https://doi.org/10.1038/srep37786>.
- [25] Valle-Maroto SM, Barreiro-Iglesias A, Fernández-López B, Rodicio MC. Data on the recovery of glycinergic neurons after spinal cord injury in lampreys. *Data Brief* 2020;28. <https://doi.org/10.1016/j.dib.2019.105092>.
- [26] Sobrido-Cameán D, Yáñez-Guerra L, Robledo D, López-Varela E, Rodicio MC, Elphick MR, Anadón R, Barreiro-Iglesias A. Cholecystokinin in the central nervous system of the sea lamprey *Petromyzon marinus*: precursor identification and neuroanatomical relationships with other neuronal signalling systems. *Brain Struct Funct* 2020;225. <https://doi.org/10.1007/s00429-019-01999-2>.
- [27] Sobrido-Cameán D, González-Llera L, Anadón R, Barreiro-Iglesias A. Organization of the corticotropin-releasing hormone and corticotropin-releasing hormone-binding protein systems in the central nervous system of the sea lamprey *Petromyzon marinus*. *J Comp Neurol* 2023;531. <https://doi.org/10.1002/cne.25412>.
- [28] González-Llera L, Sobrido-Cameán D, Santos-Durán GN, Barreiro-Iglesias A. Full regeneration of descending corticotropin-releasing hormone axons after a complete spinal cord injury in lampreys. *Comput Struct Biotechnol* 2022;20. <https://doi.org/10.1016/j.csbj.2022.10.020>.
- [29] Ohta Y, Brodin L, Hökfelt T, Walsh JH. Possible target neurons of the reticulospinal cholecystokinin (CCK) projection to the lamprey spinal cord: immunohistochemistry combined with intracellular staining with lucifer yellow. *Brain Res* 1988;445. [https://doi.org/10.1016/0006-8993\(88\)91207-3](https://doi.org/10.1016/0006-8993(88)91207-3).
- [30] Parker D. Presynaptic and interactive peptidergic modulation of reticulospinal synaptic inputs in the lamprey. *J Neurophysiol* 2000;83. <https://doi.org/10.1152/jn.2000.83.5.2497>.
- [31] Barreiro-Iglesias A, Zhang G, Selzer ME, Shifman MI. Complete spinal cord injury and brain dissection protocol for subsequent wholemount in situ hybridization in larval sea lamprey. *J Vis Exp* 2014;14. <https://doi.org/10.3791/51494>.
- [32] Ayers J. Recovery of oscillator function following spinal regeneration in the sea lamprey. *Cell Neuron Oscil N Y Marcel Dekker* 1989;349–83.
- [33] Hoffman N, Parker D. Interactive and individual effects of sensory potentiation and region-specific changes in excitability after spinal cord injury. *Neuroscience* 2011;199. <https://doi.org/10.1016/j.neuroscience.2011.09.021>.
- [34] Mathis A, Mamidanna P, Cury KM, Abe T, Murthy VN, Mathis MW, Bethge M. DeepLabCut: markerless pose estimation of user-defined body parts with deep learning. *Nat Neurosci* 2018;21. <https://doi.org/10.1038/s41593-018-0209-y>.
- [35] Buckley K, Kelly RB. Identification of a transmembrane glycoprotein specific for secretory vesicles of neural and endocrine cells. *J Cell Biol* 1985;100. <https://doi.org/10.1083/jcb.100.4.1284>.
- [36] Lau BYB, Folds AE, Alieva NO, Oliphant PA, Busch DJ, Morgan JR. Increased synapsin expression and neurite sprouting in lamprey brain after spinal cord injury. *Exp Neurol* 2011;228. <https://doi.org/10.1016/j.expneurol.2011.02.003>.
- [37] Busch DJ, Morgan JR. Synuclein accumulation is associated with cell-specific neuronal death after spinal cord injury. *J Comp Neurol* 2012;520. <https://doi.org/10.1002/cne.23011>.
- [38] Hanslik KL, Allen SR, Harkenrider TL, Fogerson SM, Guadarrama E, Morgan JR. Regenerative capacity in the lamprey spinal cord is not altered after a repeated transection. *PLoS ONE* 2019;14. <https://doi.org/10.1371/journal.pone.0204193>.
- [39] Fouke KE, Wegman ME, Weber SA, Brady EB, Román-Vendrell C, Morgan JR. Synuclein regulates synaptic vesicle clustering and docking at a vertebrate synapse. *Front Cell Dev Biol* 2021;9. <https://doi.org/10.3389/fcell.2021.774650>.
- [40] Reymann J. LIGHTNING: Image Information Extraction by Adaptive Deconvolution [White paper] 2018. Leica Microsystems.
- [41] Fernández-López B, Valle-Maroto SM, Barreiro-Iglesias A, Rodicio MC. Neuronal release and successful astrocyte uptake of aminoacidic neurotransmitters after spinal cord injury in lampreys. *Glia* 2014;62. <https://doi.org/10.1002/glia.22678>.
- [42] Lurie DI, Pijak DS, Selzer ME. Structure of reticulospinal axon growth cones and their cellular environment during regeneration in the lamprey spinal cord. *J Comp Neurol* 1994;344. <https://doi.org/10.1002/cne.903440406>.
- [43] Zhang G, Rodemer W, Sinita I, Hu J, Selzer ME. Source of early regenerating axons in lamprey spinal cord revealed by wholemount optical clearing with BABB. *Cells* 2020;9. <https://doi.org/10.3390/cells9112427>.
- [44] Selzer ME. Mechanisms of functional recovery and regeneration after spinal cord transection in larval sea lamprey. *J Physiol* 1978;277. <https://doi.org/10.1113/jphysiol.1978.sp012280>.
- [45] Davis GR, Troxel MT, Kohler VJ, Grossmann EM, McClellan AD. Time course of locomotor recovery and functional regeneration in spinal-transected lamprey: kinematics and electromyography. *Exp Brain Res* 1993;97. <https://doi.org/10.1007/BF00228819>.
- [46] Katz HR, Fouke KE, Losurdo NA, Morgan JR. Recovery of burrowing behavior after spinal cord injury in the larval sea lamprey. *Biol Bull* 2020;239. <https://doi.org/10.1086/711365>.
- [47] Rovainen CM. Regeneration of Muller and Mauthner axons after spinal transection in larval lampreys. *J Comp Neurol* 1976;168. <https://doi.org/10.1002/cne.901680407>.
- [48] Bertels H, Vicente-Ortiz G, El Kanbi K, Takeoka A. Neurotransmitter phenotype switching by spinal excitatory interneurons regulates locomotor recovery after spinal cord injury. *Nat Neurosci* 2022;25. <https://doi.org/10.1038/s41593-022-01067-9>.
- [49] Lamanna F, Hervas-Sotomayor F, Oel AP, et al. A lamprey neural cell type atlas illuminates the origins of the vertebrate brain. *Nat Ecol Evol* 2023;7. <https://doi.org/10.1038/s41559-023-02170-1>.
- [50] Kuljis RO, Karten HJ. Regeneration of peptide-containing retinofugal axons into the optic tectum with reappearance of a substance P-containing lamina. *J Comp Neurol* 1985;240. <https://doi.org/10.1002/cne.902400102>.
- [51] Shifman MI, Zhang G, Selzer ME. Delayed death of identified reticulospinal neurons after spinal cord injury in lampreys. *J Comp Neurol* 2008;510. <https://doi.org/10.1002/cne.21789>.
- [52] Shifman MI, Selzer ME. Differential expression of class 3 and 4 semaphorins and netrin in the lamprey spinal cord during regeneration. *J Comp Neurol* 2007;501. <https://doi.org/10.1002/cne.21283>.
- [53] Laramore C, Maymind E, Shifman MI. Expression of neurotrophin and its tropomyosin-related kinase receptors (Trks) during axonal regeneration following spinal cord injury in larval lamprey. *Neuroscience* 2011;183. <https://doi.org/10.1016/j.neuroscience.2011.03.024>.
- [54] Shifman MI, Selzer ME. Expression of the netrin receptor UNC-5 in lamprey brain: modulation by spinal cord transection. *Neurorehabil Neural Repair* 2000;14. <https://doi.org/10.1177/154596830001400106>.
- [55] Barreiro-Iglesias A, Laramore C, Shifman MI. The sea lamprey UNC5 receptors: cDNA cloning, phylogenetic analysis and expression in reticulospinal neurons at larval and adult stages of development. *J Comp Neurol* 2012;520. <https://doi.org/10.1002/cne.23143>.
- [56] Shifman MI, Yumul RE, Laramore C, Selzer ME. Expression of the repulsive guidance molecule RGM and its receptor neogenin after spinal cord injury in sea lamprey. *Exp Neurol* 2009;217. <https://doi.org/10.1016/j.expneurol.2009.02.011>.
- [57] González-Llera L, Shifman MI, Barreiro-Iglesias A. Neogenin expression in ependymo-radial glia of the larval sea lamprey *Petromyzon marinus* spinal cord. *MicroPubl Biol* 2023;2023. <https://doi.org/10.17912/micropub.biology.000810>.

- [58] Fies J, Gemmell BJ, Fogerson SM, Morgan JR, Tytell ED, Colin SP. Swimming kinematics and performance of spinal transected lampreys with different levels of axon regeneration. *J Exp Biol* 2021;224. <https://doi.org/10.1242/jeb.242639>.
- [59] Sobrido-Cameán D, Barreiro-Iglesias A. Morpholino studies shed light on the signaling pathways regulating axon regeneration in lampreys. *Neural Regen Res* 2022;17. <https://doi.org/10.4103/1673-5374.330597>.
- [60] McClellan AD. Brainstem command systems for locomotion in the lamprey: localization of descending pathways in the spinal cord. *Brain Res* 1988;457. [https://doi.org/10.1016/0006-8993\(88\)90704-4](https://doi.org/10.1016/0006-8993(88)90704-4).